Featured in Physics

Emergence of Complex Network Topologies from Flow-Weighted Optimization of Network Efficiency

Sebastiano Bontorin,[1,2] Giulia Cencetti,[1] Riccardo Gallotti,[1] Bruno Lepri,[1] and Manlio De Domenico[3,4,5,*]

[1]*Fondazione Bruno Kessler, Via Sommarive 18, 38123 Povo (TN), Italy*
[2]*Department of Physics, University of Trento, Via Sommarive 14, 38123 Povo (TN), Italy*
[3]*Department of Physics and Astronomy "Galileo Galilei", University of Padua, Via F. Marzolo 8, 315126 Padova, Italy*
[4]*Padua Center for Network Medicine, University of Padua, Via F. Marzolo 8, 315126 Padova, Italy*
[5]*Istituto Nazionale di Fisica Nucleare, Sez. Padova, Italy*

(Received 20 January 2023; revised 13 February 2024; accepted 29 April 2024; published 21 June 2024)

Transportation and distribution networks are a class of spatial networks that have been of interest in recent years. These networks are often characterized by the presence of complex structures such as central loops paired with peripheral branches, which can appear both in natural and manmade systems, such as subway and railway networks. In this study, we investigate the conditions for the emergence of these nontrivial topological structures in the context of human transportation in cities. We propose a simple model for spatial networks generation, where a network lattice acts as a planar substrate and edge speeds define an effective temporal distance which we aim to optimize and quantifies the efficiency in exploring the urban space. Complex network topologies can be recovered from the optimization of edges' speeds and we study how the interplay between a flow probability between two nodes in space and the associated travel cost influences the resulting optimal network. In the perspective of urban transportation we simulate these flows by means of human mobility models to obtain origin-destination matrices. We find that when using simple lattices, the obtained optimal topologies transition from treelike structures to more regular networks, depending on the spatial range of flows. Remarkably, we find that branches paired to large loops structures appear as optimal structures when the network is optimized for an interplay between heterogeneous mobility patterns of small range travels and longer-range ones typical of commuting. Moreover, when congestion dynamics in traffic routing is considered, we study the emergence of additional edges from the tree structure to mitigate temporal delays. Finally, we show that our framework is able to recover the statistical spatial properties of the Greater London area subway network.

DOI: 10.1103/PhysRevX.14.021050

Subject Areas: Complex Systems, Computational Physics, Statistical Physics

I. INTRODUCTION

Cities represent one of the most fascinating manmade complex systems, exhibiting complex features ranging on different scales: from their structure and dynamical behavior, up to the scaling of socioeconomic factors with their size [1–5]. These features represent a strong hint toward the existence of universal underlying mechanics behind apparently very different cities [6–8]. Out of these structural properties, one of the most relevant, as it plays a fundamental role mediating the complex interplay between human dynamics [9,10] and mobility in urban context, is transportation networks [11–15]. These networks are a class of spatial networks whose properties have been investigated in the literature during the past two decades [14,16]. In particular, they have been studied under the lens of optimality conditions and minimization of cost-based functionals [16], in order to identify specific features behind efficient networks. The concept of optimal networks [2] and energylike minimization [17] has its natural understanding in the physics language. States of a system which minimize a functional defining trade-off between system's observables (e.g., free energy) represent the most likely to be observed states of many real world systems. While in some complex systems, such as cities, these physical variables cannot be derived from first principles, these analogies and concepts can still offer a valid perspective and provide an embedding of these systems in a space where the interplay between their structure and dynamics

*Corresponding author: manlio.dedomenico@unipd.it

can be unfolded and better understood. Simple laws have been studied [16,18] to better understand the emergence of hierarchy and the role of traffic in the network state. Moreover, global and local optimization criteria lie in the evolution of manmade systems where policymakers and planners can adopt some of these criteria in their plans [14].

Transportation networks are often characterized by the presence of complex structures [19–21] such as loops paired with branches [22], which can appear both in natural [23] and manmade systems [14], like railway and subway networks. These structures represent the key topological elements behind efficient public transportation systems [20]. In this study we devise a theoretical framework in the domain of network science, aimed to investigate optimal network features with parsimonious modeling choices, rather than directly inform urban planning. We first explore the transitions from tree networks to latticelike structures and ultimately investigate the conditions for the emergence of the aforementioned nontrivial structures [18,24] in the context of human transportation in cities [25]. We aim to reconstruct these topologies by means of an optimal configuration [26,27] of the network state. Under the assumption of a fixed total cost and a limited set of high-capacity connections (e.g., a constraint in the expenditure available on infrastructure), the optimal configuration is the assignation of connections' speeds, or edges' weights, such that the joint amount of time required to travel between two nodes is minimized for all pairs of nodes. Moreover, as these networks represent the arteries in urban exploration and navigation via public transportation, we study the role of flows between node pairs [18,28] as a traffic that defines the importance of specific network paths. We model the urban spatial features which generate heterogeneous distributions of human mobility in space, biasing these optimal networks to converge toward specific topological structures. In the context of spatial network science, we aim to explore the minimum requirements and the conditions for these optimization processes to reproduce the empirical structures aforementioned. Albeit this theoretical abstraction allows us to embed mechanisms such as human mobility [10] and congestion [29], more complex elements such as mode choice, trip frequency, and other fundamental aspects in urban planning [30] are not considered. Thus, it provides insights from a network science perspective applied to transportation in urban systems.

At variance with the recent works on network efficiency and transportation topologies, we adopt some fundamentally different modeling choices. We evaluate the efficiency in terms of time necessary to explore the network, where edges' weights w_e act as travel speeds. We optimize these speeds in a continuous interval, instead of using a multilayer constraint or specific topologies [27,31]. We also weight path travel time by the traffic probability between nodes. In this work we call the network $G(\{w_e\})$ "optimal" if the configuration of speeds $\{w_e\}$ minimizes the flow-weighted temporal distance [as defined in Eq. (2)]. Consequently, we regard the optimal network G as "efficient" when it provides the fastest travel time for the set of flows. We remark that definition of optimality in applied transport planning may differ based on the specific target [32].

The underlying network lattice (as represented in its simplest form by the triangular lattice in the next sections) acts as a planar substrate that allows the network to evolve [31,33] and possibly exhibit the network topological features typical to real world systems. On this framework, we show how introducing simple probabilities biasing the optimal efficiency between points in space forces a transition between a treelike topology and a network resembling a simple lattice. Moreover, we also discuss in Sec. IV the effect of introducing travelers' behaviors in choosing the route between origin and destination, following concepts such as user equilibrium (UE) and congestion dynamics [29,34–36]. We implement traffic routing under these conditions in the optimization of the substrate's edges, highlighting a transition from the tree structure to a multiple-pathways structure necessary to mitigate the temporal delays introduced by congestion effects. We show also that the modeling of flows resembling human mobility patterns forces the emergence of preferential shared paths in the planar substrate, whose complex topologies ultimately show features observed in real systems. Features such as a bimodality in the edges' speeds distribution, characteristic of multilayered transportation, and the central core with loops paired with branches typical of subway systems [20,22] are recovered. We finally show an application of the model within the Greater London area (GLA), finding similarities of the optimal model with its London underground network.

II. FRAMEWORK FOR URBAN SPATIAL STRUCTURE

We introduce here a general framework for spatial networks with the aim of recovering a simple model for urban structures that encodes both transportation properties and urban features such as population and density of points of interest (POIs). To this aim, we begin from the definition of a network substrate which acts as an effective discretization of the spatial dimension. Its simplest form can be found in a hexagonal two-dimensional tiling [37] and its planar dual, the triangular lattice. More formally, in this network substrate each tile in space is represented by a node, connected to its set of neighboring nodes (see Fig. 1). The existence of a physical edge between nodes and tiles i and j is encoded in the adjacency matrix A where $A_{ij} = 1$ if the regions are neighbors in the lattice. Distances and metrics are therefore computed on top of this network substrate.

Nodes of this network can encode spatial features at the urban scale, such as population or amenities' density in a given node. We therefore have a simple representation of an urban spatial structure (see Fig. 1), and a network substrate that can be optimized to generate planar transportation networks which are optimized for flow efficiency based on

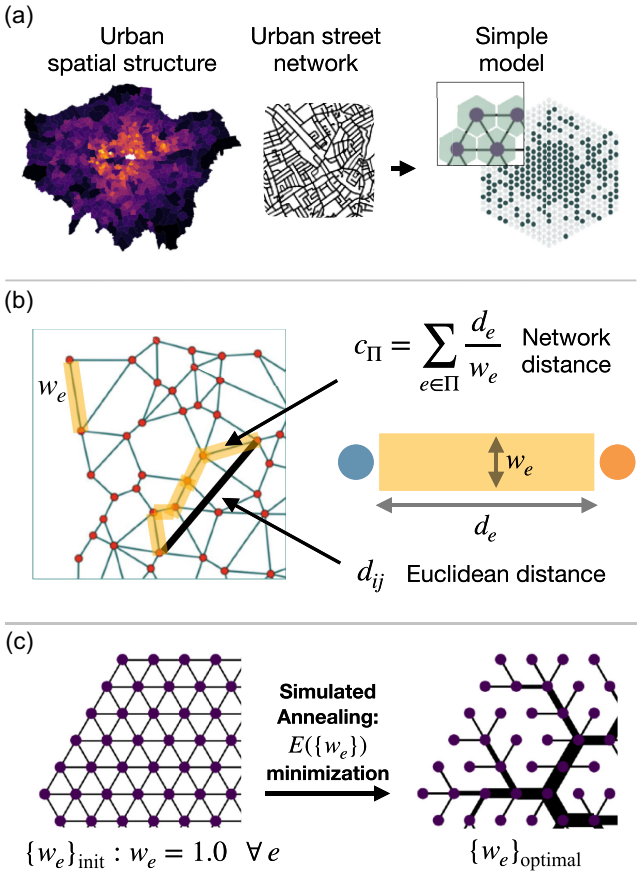

FIG. 1. Spatial network model for urban structure. (a) Mapping population distribution and urban transportation network to a spatial network where nodes encode urban features. Example with hexagonal tiling mapped to the triangular lattice. (b) Network-based distance $c_{\Pi_{ij}}$ versus Euclidean distance d_{ij}; edges' weights and speeds w_e are depicted as widths. (c) Edges' weights of the lattice substrate are optimized via simulated annealing to unravel spatial features of the optimal transportation network which guarantees the highest flow efficiency evaluated as minimum travel time.

the travel time [33]. The path-based temporal distance on top of the transportation network acts as the fundamental metric we aim to minimize. The rationale behind a network-based distance is grounded on the assumption that in the context of public transportation, urban systems are not navigated by considering geographical distance but rather by evaluating the travel time between departure and arrival. More specifically, multilayer transportation networks [11,21] are characterized by layers having a hierarchical organization with different characteristic speeds [38]. Thus, an effective temporal distance becomes fundamental in determining accessibility and efficiency in urban space exploration.

In this model, we denote e as an edge in the network and w_e as the associated edge's weight which can be seen as the connection's speed in the transportation network. d_e is the Euclidean distance of edge e between the nodes it is connecting; here, edge weights or speeds are visually mapped as widths of the links. Information about edges' distance in this framework can be relevant when generalizing to the case of random spatial networks where edges have different lengths. In the case of a general nonspatial network, where there is no notion of spatial distances, the model can be adapted by fixing $d_e = 1$. Finally, we define $\Omega_{\Pi_{ij}}$ as the set of paths connecting the two nodes. We then maximize the efficiency of this underlying substrate. The transportation efficiency between two nodes $i - j$ is computed as a cost in terms of time [39]. We first do not consider the route assignment for each pair $i - j$ dependent on congestion dynamics [29] but rather on the "all-or-nothing" paradigm, finding the shortest path. In Sec. IV we also route traffic following user equilibrium [29,34] in the optimization process and discuss the effect on simple topologies. Therefore, we find the path (a set of connected edges starting from source node i and ending in destination node j) with the smallest cumulative time, independently by the routing of other flows on the network. We consider an edge e's weight w_e as a proxy of the edge's travel speed. Hence, given the edge's length d_e, we have that d_e/w_e is the effective travel time on edge e. See Fig. 1 for a graphic depiction. Here $G(\{w_e\})$ is used to indicate the network G with configuration of edges' travel speeds $\{w_e\}$. We therefore aim to find the assignment of speeds $\{w_e\}$ which minimize the set of travel times $\{c_{ij}\}$ between pair of nodes $i - j$, where each element c_{ij} is defined as

$$c_{ij}(\{w_e\}) = \min_{\Pi\in\Omega_{\Pi_{ij}}} \left[\sum_{e\in\Pi_{ij}} \frac{d_e}{w_e}\right], \tag{1}$$

and in absence of further information, the optimization procedure is the equivalent of minimizing the cumulative travel times $\sum_{ij} c_{ij}$. Here we add a novel ingredient, in which we couple the optimization of the network temporal distances with a traffic flow or travel probability between pairs of nodes. Operationally, when dealing with real world origin-destination (OD) matrices, this probability can then be mapped to a flow T_{ij} between two points. T_{ij} may represent the probability of a person from node i to travel to node j, and traffic resembling human mobility flows can be recovered when information about populations in source and target nodes is added. T_{ij} effectively acts as a rank in the importance of a specific path in the network. As paths connecting different pairs of nodes may share common edges of the network substrate, complex topologies emerge from the shared paths jointly optimizing the network efficiency. The flow-weighted network effective travel time therefore becomes

$$E(G(\{w_e\})) = \frac{1}{N(N-1)} \sum_{i}^{N} \sum_{j\neq i}^{N} T_{ij} \cdot c_{ij}(\{w_e\}). \tag{2}$$

We also require that the total network infrastructure cost, defined as the cumulative sum of edges' weights per unit

length multiplied by edge distance $C_G = \sum_{e \in G} d_e w_e$, is conserved. Equation (2) can be seen as a generalization of a standard optimization process, in the sense that when $T_{ij} = 1, \ \forall \ (i,j)$, the efficiency is optimized for all possible trip pairs (i,j) with equal importance, where treelike topologies often represent the optimal solution [14]. In Sec. IV we also discuss the case of routing traffic flows T_{ij} following user equilibrium conditions and not just taking the shortest path. This traffic assignment process allows us to explore the effect of congestion dynamics in the generation of optimal topologies on simple spatial networks.

Before tackling the problem of flows characterized by human mobility patterns [10], we study a simpler definition of T_{ij}. This allows us to understand the role of distance d_{ij} in the optimization process, in the absence of other nodes' features:

$$T_{ij} \propto e^{-\beta d_{ij}}. \tag{3}$$

The coefficient β appearing in Eq. (3) is introduced as a penalizing parameter and determines how relevant is the pairwise distance d_{ij} when computing probabilities. We can understand it as the inverse of a characteristic traveling distance for an agent on the network $\beta \sim (1/d_0)$. While several alternatives on the integration of distance in spatial-dependent probabilities (such as power laws $T_{ij} \sim d_{ij}^{-\gamma}$) can be employed, we focus on the exponential dependence as it represents the foundational result from the maximum entropy derivation of gravity flows [40]. The introduction of gravitylike flows will be discussed in Sec. V.

In the following, we introduce the application of the model on simple substrates to explore the role of β in absence of spatial urban features.

III. OPTIMIZATION OF SIMPLE NETWORK SUBSTRATES

In order to asses the role of the characteristic distance parameter β in the emergence of specific topologies, we compute networks statistics on a set of generative models for both spatial and nonspatial networks. As hexagonal tiling of space is preferable when an analysis includes aspects of connectivity [37], the first model we study is a triangular lattice. The reason behind this choice is that it represents the planar dual [14,41] of the hexagonal lattice. Therefore, as space is discretized in hexagonal tiles, the spatial network connecting its centers is the triangular lattice, which is isotropic and presents less equivalent degenerate paths of a rectangular lattice. As a direct reference to hexagonal tiling, we refer to this network as HEX (see Fig. 2). We also extend the analysis to the case of a random network model where nodes are not embedded in a metric space. Specifically, we study an Erdős-Rényi (ER) network topology, where the definition of distance between nodes L_{ij} can be defined in terms of topological shortest path distance [42].

As a first benchmark we simplify flows as a spatial probability $T_{ij} = p_{ij}$ that decays exponentially with distance and does not consider nodes features. The resulting equation for p_{ij} is

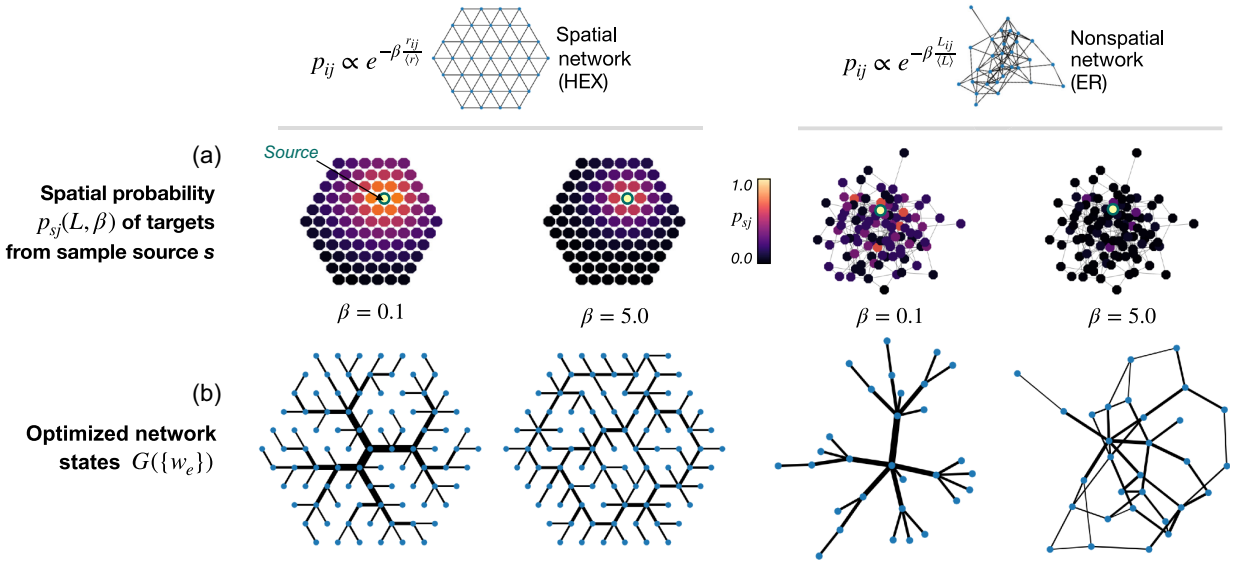

FIG. 2. Optimization of synthetic networks. The role of β is studied for two network models: the triangular lattice (HEX) and the nonspatial (ER) network. (a) Heat map of target nodes probabilities p_{ij} from source node (yellow) under two different β values: As the penalty parameter grows, farther nodes are more penalized and flows tend to stay close to the source. (b) Samples of the associated optimized network states: When flows are not affected by distances ($\beta = 0.1$), source nodes target all the other nodes in the network with approximately equal probability, the optimal network converges to a treelike structure. With larger β ($\beta = 5.0$), trip probabilities are more localized and the presence of loops appears in the optimal structure.

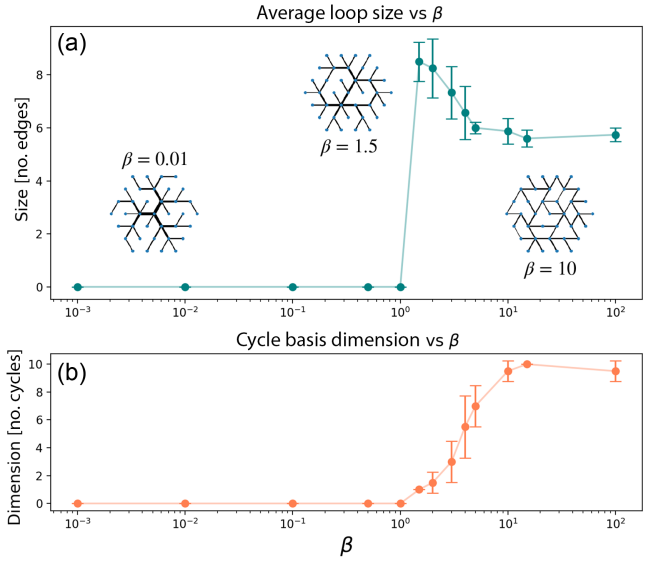

FIG. 3. Loop dimension versus β. Minimum cycle basis is used as a network's observable to study the appearance of loops. For each point the median and its absolute deviation are shown. (a) The average size (number of edges) of the loops that constitute the cycle basis. (b) Cycle basis dimension as number of loops. The topology that minimizes the flow-weighted travel time ranges from a tree structure to a latticelike with small loops, as the probability of long-range movement decreases (large β). A transition in the cycle basis property is observed at $\beta \sim 1.0$ for the triangular lattice under study, where the optimal network results in an intermediate state with large loops.

$$p_{ij} = \frac{e^{-\beta d_{ij}/\langle d\rangle}}{\sum_{k\neq i}^{N-1} e^{-\beta d_{ik}/\langle d\rangle}}, \tag{4}$$

where $\langle d\rangle = [1/N(N-1)]\sum_{i\neq j} d_{ij}$ is the average distance of points in the network and acts as a normalization factor (Euclidean distance $\langle r\rangle$ in case of a spatial network or topological $\langle L\rangle$ for the ER network).

Therefore, p_{ij} encodes how much of the nearby space is explored by a single source node. An illustration of the spatial dependence of target probabilities and samples of the resulting optimal topologies are presented in Fig. 2.

For a range of β values the optimization process is performed on an ensemble of these models. To assess the emergence of complex structures we observe the number of loops that emerge in the optimal state. This measure is relevant in the context of spatial networks, where loops break the symmetry introduced by optimal structures such as trees. We compute the minimum cycle basis set as a metric to observe the emergence of loops [43]: i.e., the minimum set of loops (where a single loop is encoded in a set of edges that defines a closed path in the graph) such that any other closed path in the network can be reconstructed via combination of this cycle basis [43]. Specifically, we investigate the cycle basis dimension (the number of loops that constitute this set) and the average loop size, against a range of β values. This metric allows us to quantify the emergence of spatial topological features that differentiate the optimal state from a tree structure. Results for these synthetic systems are presented in Fig. 3. Additional box plots are shown in Supplemental Material (SM) Figs. 1 and 2 [44]. A treelike topology is recovered when the flow probabilities are distributed uniformly across all nodes in space [when $\beta \to 0$ and distance is therefore not a penalizing variable in Eq. (4)], while loops emerge when farther targets become less likely to be explored and the network is globally optimized for close-range trips. Notably, in Fig. 3 around $\beta \approx 1.0$, we observe a sharp transition in the average loop size in the HEX lattice under analysis: Connections appear between neighboring nodes which are far from the tree root as it becomes more efficient to have a direct link. In this β regime the tree topology does not guarantee the most efficient configuration for peripheral nodes, which have their high probability targets in their direct neighborhood [see Eq. (4)]. Thus, in the optimization process edges appear between leaves nodes which are in separated branches: This ultimately breaks the tree structure and leads to the emergence of large-scale loops. Eventually the most efficient network converges to a simpler structure with small loops as the network is optimized for nodes to target only direct neighbors in the lattice. Finally, in SM Sec. II [44] we show an application of the case of a single target node in the perimeter of the lattice, where the model reproduces leaves venation patterns [14,45].

IV. TRAFFIC CONGESTION IN THE GENERATION OF OPTIMAL TOPOLOGIES

In this section we discuss the outcome of routing traffic T_{ij} following concepts of user equilibrium (and not following the all-or-nothing paradigm [34] of taking the shortest path in time) during the process of annealing and generation of the optimal configuration of network speeds $\{w_e\}$. We provide more detailed analytical derivations in Sec. III in SM [44]. At variance with the "free-flow" [29] time t_0 optimized in Eq. (1) where edge travel time was $t_0 = d_e/w_e$, we here assume that traffic routing generates a delay in each edge travel time via congestion dynamics. This is often modeled [34] via the Bureau of Public Roads function:

$$t_e = t_0 \cdot \left[1 + \alpha\left(\frac{T_e}{c_e}\right)^{\lambda}\right], \tag{5}$$

where T_e is the total traffic flow on edge e, c_e the edge capacity, and α, λ parameters governing the nonlinearity of congestion. OD traffic is then assigned on the network following user equilibrium conditions given the network configuration $G(\{w_e\})$ [29,34]. We first consider the capacity as constant $c_e = 1.0$.

We start by considering the benchmark network of treelike topologies obtained by optimizing flows in

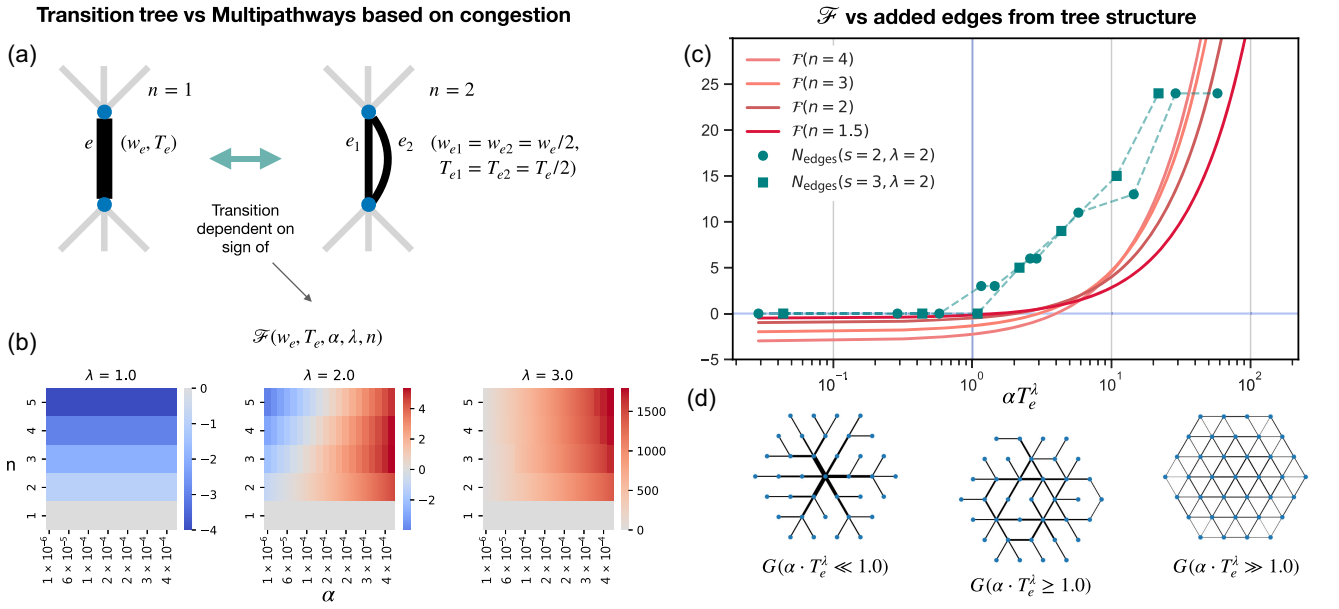

FIG. 4. Transition between topologies under congestion dynamics and analytical dependency. We study the transition from tree structure to multipathways topologies as optimal networks when traffic routing is affected by congestion mechanics. (a) Simple case where the largest-load edge in a tree structure is compared in efficiency versus an n-pathways alternative ($n = 2$ here). (b) This allows an analytical derivation [Eq. (8)] of function $\mathcal{F}$ whose sign determines which of the configurations is more favorable under different parameters. A more detailed discussion is also present in SM Sec. III [44]. (c) Plot of the emergence of additional pathways encoded in $n > 1$ from the G^{tree} versus the value of $\mathcal{F}$. Plotting the curves for different parameters and triangular lattice sizes s (see SM Sec. III) against αT_e^λ shows the collapse of curves in a common transition. We plot analytical curves $\mathcal{F}(\lambda = 2)$ for different n and highlight the threshold $\alpha T_e^\lambda = 1.0$ after which $\mathcal{F}(\lambda = 2, n > 1) > 0$, therefore predicting the emergence of new edges from the tree structure encoded in N_{edges}. (d) Resulting topologies in the case of $s = 3, \lambda = 2$. Specifically for $\alpha T_e^\lambda \ll 1.0, \geq 1.0, \gg 1.0$. We can appreciate the regimes in which the tree structure transitions to a complete lattice. This is a consequence of $\mathcal{F}(n, \alpha, T_e, \lambda)$ that for large nonlinearity parameter λ and relevance of congestion α favors large n and therefore the decomposition of traffic in as many pathways as possible in the lattice.

Eq. (4) with $\beta = 0$. As the strength of congestion increases, we expect the tree structure to transition to a structure where multiple pathways between node pairs $i - j$ emerge to sustain the congestion as optimal features. We analytically study the condition for the highest-load (T_e) edge in the tree to be a more favorable structure than an n-edges alternative structure. This happens when the efficiency (traffic-weighted travel time) of a single edge with speed w_e carrying the maximum traffic T_e ($n = 1$) is lower than the efficiency of the decomposition of traffic on a set of n edges ($\mathcal{N}_e$) given the congestion state [Eq. (8)]. We can decompose Eq. (2), after the traffic assignment procedure, as a sum of edges' efficiencies $E = \sum_e E_e = \sum_e T_e \cdot t_e$ (see SM Sec. III [44]). This allows us to detach the study of efficiency on a single edge of relevance (such as the largest traffic edge in a tree network). We therefore study the inequality:

$$E_e[T_e, w_e, (\lambda, \alpha)] \leq \sum_{e \in \mathcal{N}_e} E_e \left[\frac{T_e}{n}, \frac{w_e}{n}, (\lambda, \alpha)\right], \qquad (6)$$

where we force the constraints on w_e and T_e to be conserved quantities. This case is depicted in Fig. 4(a), and in SM Sec. III we describe the full derivation. The inequality can be ultimately rewritten as

$$\frac{T_e}{w_e} \cdot \left[(1 - n) + \alpha T_e^\lambda \left(1 - \frac{1}{n^{\lambda - 1}}\right)\right] \leq 0, \qquad (7)$$

$$\frac{T_e}{w_e} \cdot \mathcal{F}(n, \alpha, T_e, \lambda) \leq 0, \qquad (8)$$

where we have condensed the inequality in the function $\mathcal{F}(n, \alpha, T_e, \lambda)$ whose sign determines whether it is more favorable ($\mathcal{F} < 0$) for a single edge to carry the traffic load under the set of parameters. Instead, when $\mathcal{F} > 0$, the inequality is not satisfied and the n-pathways structure is more efficient (lower traffic-weighted temporal cost t_e) and multiple pathways emerge to alleviate the temporal delays introduced by congestion on the single edge. In Fig. 4(b) the values of $\mathcal{F}$ identify different regimes at varying the nonlinearity in the congestion term given by parameter λ. Interestingly, the tree structure represents the optimal $G(\{w_e\})$ even with $\lambda = 1$, a scenario where congestion mechanics is present, but linearly dependent on T_e. For $\lambda = 2$ we observe a transition in the optimality of n pathways as congestion intensity α increases. Moreover, when $\lambda = 3$,

in the range of α presented in Fig. 4 the n pathways is instead the optimal topological feature. In Fig. 4(c) we better investigate the transition by generating the optimal network states on HEX lattices. We compute the number of additional edges from the tree structure $N_{\text{edges}} = N_{\text{edges}}(G) - N_{\text{edges}}(G^{\text{tree}})$ as a function of the congestion parameters versus the rescaled control parameter αT_e^{λ} for different network sizes (s) and λ, comparing with the change in sign of the functional $\mathcal{F}$. We remark that albeit Eq. (8) represents a simple approximation scenario, this functional can approximate the transition for different network sizes and of congestion parameters varying different orders of magnitudes. We observe the transition from treelike structure to a complete lattice, also visible in the topologies [Fig. 4(d)]. Moreover, in SM Sec. III we show how the joint optimization of edge speed w_e and capacity (by modeling $c_e = w_e$) leads to the tree being a stable structure in any congestion scenario ($\mathcal{F} < 0$) [44].

V. SPATIAL ATTRACTIVENESS AND FLOWS MODELING HUMAN MOBILITY PATTERNS

In the context of urban systems, optimal transportation networks need to be devised to accommodate traffic flows [28] toward specific areas of interest, e.g., due to high commercial and business land use density. Hence we extend the efficiency optimization framework in the case where we have T_{ij} flows that mimic human mobility patterns on top of the urban networks, as the presence of nodes with high attractiveness (POIs) biases the flows toward them. In urban scenarios we adopt spatial-interaction models to generate these flows. In these models, flows are obtained via a gravitylike equation, $T_{ij} \propto p_i p_j \exp(-\beta d_{ij})$ [10], which can be derived from first principles via entropy maximization, thus representing the most likely set of flows to be observed given the constraints. While several models [10] can be in principle employed to model local mobility decisions [46] or hierarchical mobility properties [47], recent works have shown the validity of gravitylike models [48]. Moreover, in the context of urban exploration, the gravity equation can be mapped to a model for spatial interaction [40,49] where nodes with a given attractiveness W_j compete as possible targets:

$$T_{ij} \propto \frac{1}{Z} P_i W_j \exp(-\beta d_{ij}). \tag{9}$$

Normalization Z accounts for all possible trip alternatives $\sum_k W_k \exp(-\beta d_{ik})$. P_i is the population density in node i and W_j encodes a suitable definition of benefit or attractiveness of node j as a possible target [49]. T_{ij} is therefore the fraction of population in node i commuting or traveling on average to node j. To better understand the role of nodes' attractiveness, we start with the simplest assumption of equal population distribution on all nodes: $P_i = 1.0 \ \forall \ i$; we will introduce more realistic population distribution in the next section with the London case study. We highlight that the purpose behind adopting these mobility models is to capture the typical features observed

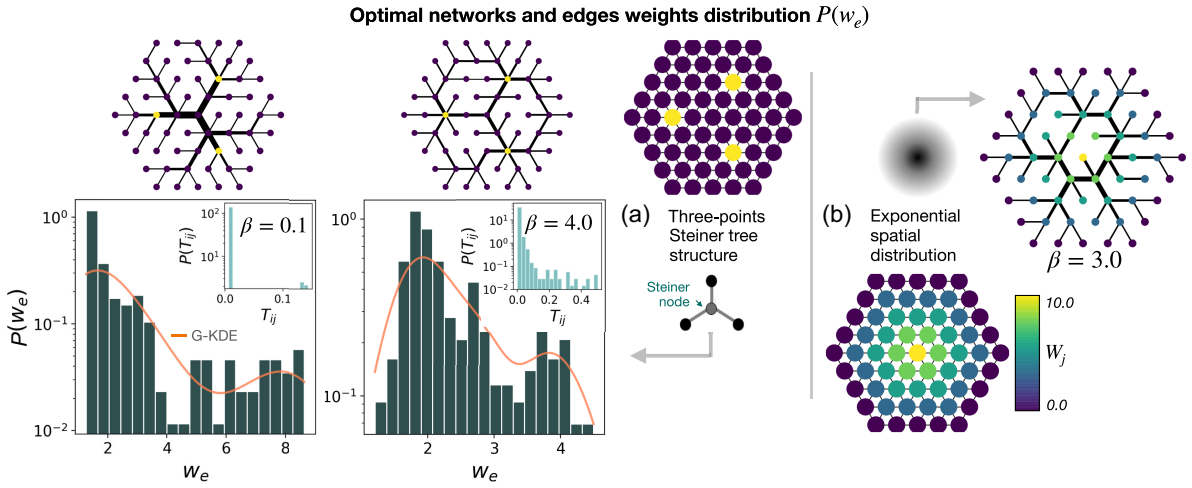

FIG. 5. Simple models of urban structure and attractiveness distributions under study (three-points and exponential decay). Spatial distribution of POIs, where attractiveness W_j is mapped with color intensity (yellow being higher). Optimized edges' weights distributions $P(\{w_e\})$ are characterized by the bimodal nature that reveals the multilayered structure of the optimal transportation networks when close-range flows are paired with long-range traffic typical of commuting toward city centers [insets: $P(T_{ij})$ with peaks on large flows due to POIs]. Gaussian Kernel density estimate (G-KDE) is shown in orange as a visual aid. (a) Three-points polycentric distribution of POIs, resembling the Euclidean Steiner tree problem [51,52] for three points. The network is optimized with $\beta = 0.1$ and $\beta = 4.0$, and shows the appearance of branches connecting the POIs paired to large loops in the periphery. (b) Optimal state and distribution of speeds with exponential decay of W_j from the center and an exemplifying result with $\beta = 3.0$. The optimal topology that minimizes the flow-weighted travel time is characterized by a central loop paired with branches.

in human mobility flows (such as the dependence on distance and the existence of attractive sinks [50]) rather than fit observed data.

We apply these models on the triangular lattice to unravel the optimal topologies that emerge when T_{ij} probabilities are biased toward some nodes having high attractiveness (simulating POIs), and we study two spatial configurations for nodes' W_j. In the first configuration high W_j is assigned to three nodes (POIs) placed at the vertices of an equilateral triangle. We study the three-points distribution as it mimics a prototypical polycentric distribution of city centers, and it can be linked to the solution of the Euclidean Steiner tree problem [51,52]. The Steiner tree is a class of problems where given a set of N points in a plane the goal is to find the set of lines connecting the points with minimum cumulative length. In our case, the solution would lie in the central node of the lattice being the Fermat point [52] and the Steiner node, which connects the three vertices of the high W_j triangle, as illustrated in Fig. 5(a). The second case is a distribution of W_j that decays exponentially from the center, mimicking a more realistic spatial distribution for a urban monocentric structure. The two spatial structures are depicted in Fig. 5.

We find that due to nodes in the network biasing the flows T_{ij}, as it can be seen in the insets of Fig. 5(a), the traffic flows get divided into two types: a close-range paired to a long-range set of flows, due to POI polarization. We show in Fig. 5 optimal solutions for values of $\beta = 0.1, 4.0$. Interestingly, optimal solutions are characterized by three central lines branching from the center (which therefore acts as Steiner node) and connecting the three nodes with high attractiveness, therefore resembling the solution of the Steiner tree problem. Moreover, in the case of more localized flows ($\beta = 4.0$) these lines are also paired with large-scale loops connecting farther nodes. We also find that the heterogeneity of T_{ij} flows forces the appearance of a second mode in the distribution of speeds w_e (see Fig. 5). The two peaks in the optimal $P(w_e)$ can be interpreted as two different levels of speed, which suggests that the entire process can be decomposed in two distinct mechanisms which can be mapped as a bilayer network: one layer at high speeds with long-range or commuting trajectories and the other one at lower w_e with short-range paths. This also suggests a possible extension of the model to multilayer networks.

VI. GREATER LONDON AREA: GENERATIVE MODEL FOR THE SUBWAY SYSTEM

We extend in this section the application of the model by integrating data from a real urban structure. Specifically, we model the urban structure of Greater London area on top of our framework and apply the efficiency optimization process with the aim of understanding if the temporal efficiency optimization of the spatial substrate paired with gravitylike flows is sufficient to yield a transportation network with similar topological features (such as a central core paired with peripheral branches [22]) as the London subway system. To extend the model to real urban scenarios, we first obtain the distribution of amenities [53] from OpenStreetMap [54] and we use this density of points in space as a proxy to estimate the attractiveness W_j of a tile. Census data for Greater London area yards from 2014 is used to recover population density P_i. These densities are then mapped to Uber's H3 tiling to recover the spatial discretization in hexagonal tiles, such that we can have

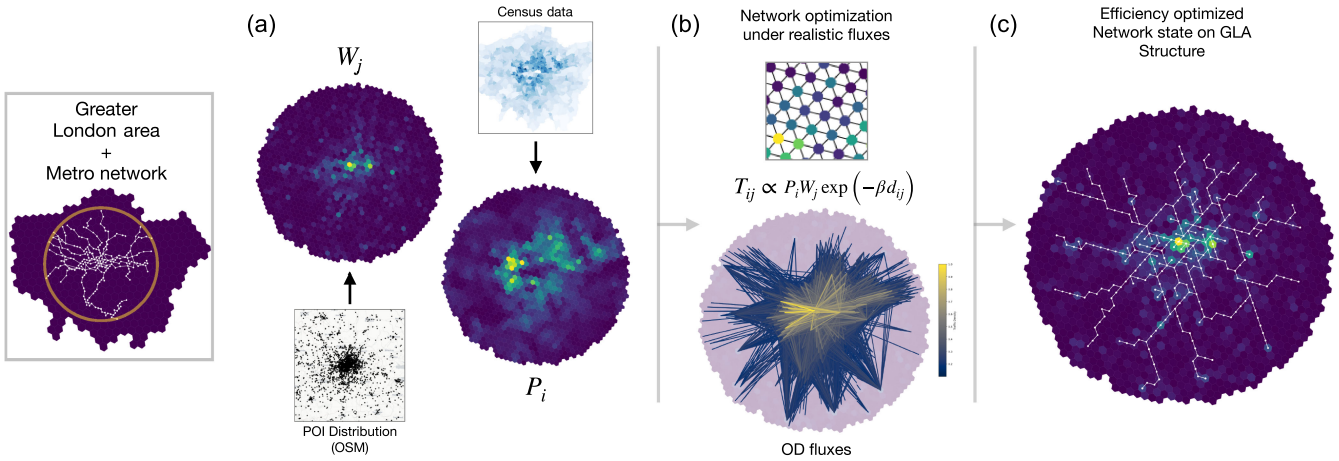

FIG. 6. Optimal network model on the Greater London area structure. Application of the efficiency optimization with flows resembling human mobility on the urban structure of the Greater London area. (a) Urban structure data are recovered from census and OpenStreetMap (OSM), and population and POI densities are mapped to the H3 tiling [55]. (b) Data is mapped to the triangular lattice, with nodes having features which allow the calculation of gravitylike flows [10,40]; a sample OD matrix is shown where T_{ij} are computed with $\beta = 0.35$. (c) Optimal network state for the London model, where only edges and nodes corresponding to the second mode are shown (see SM Sec. III [44]). The network is characterized by a central core structure with loops paired with peripheral branches.

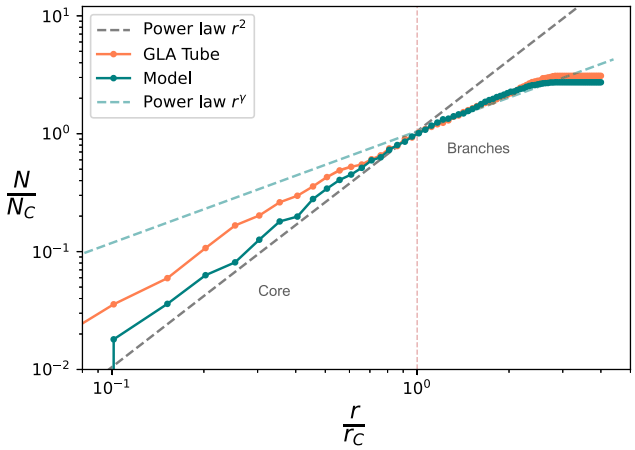

FIG. 7. Scaling properties of GLA Tube stations. Profile of the number of stations (nodes in the optimal discretized network, see SM Sec. IV [44], reproducing GLA underground) versus the distance from the barycenter. The scaling of $N(r)$ profile of the model is compared with the real network system. Scaling properties predicted in Ref. [22] are verified, finding the two different scaling regimes separated at $(r/r_C) \sim 1$ for core paired with branches systems, where r_C is the core radius (characterized by r^2 scaling), and N_C is the number of stations in the core. The scaling exponent $\gamma = 0.947 \pm 0.002$ is obtained as a linear fit of the integral curve [22] for $r > r_C$ (see SM Sec. V for more details).

direct mapping to the nodes on a triangular lattice, as in the examples discussed in previous sections. We thus have the ingredients to finally simulate the spatial interaction flows T_{ij} in Eq. (9). In Fig. 6 the integration of urban data describing London's urban structure in the model is explained and we provide a depiction of the OD matrix that arises from the spatial interaction model. With the aim of reproducing real features, we impose an upper limit on w_e, so that the distribution of weights or speeds is bounded during the optimization process: $w_e \in (0, w^*)$. This better simulates the upper bound in speed of real multilayer systems. Further explanation of data recovery and integration in the model is provided in SM Sec. IV [44]. We find (see SM Fig. 13) that $\{w_e\}$ distribution displays a bimodal shape, and this allows the analysis of the generated network in a subgraph defined by the set of high speed edges. In Fig. 6(c), we show a sample result for $\beta = 0.35$ of this subgraph. The characterization of the network into a central core paired with peripheral branches as the optimal state can be visually observed.

The model's subgraph of high speed edges is compared to the real tube network in the Greater London area [21] to assess the similarities between the optimal structure and the real subway system. We quantify this similarity by means of spatial scaling laws [22]; these are convenient to highlight the recovery of the central core structure characterized by loops, paired with quasimonodimensional lines branching from the core. We investigate the distribution of nodes stations using the profile function $N(r)$ that quantifies the total number of stations at a distance r from the network barycenter, computed as the average location of all station nodes [22]. Results of this scaling analysis for the real and simulated networks are presented in Fig. 7. The two scaling regimes indicate the separation of core and branches: the scaling of r^2 in the core center and a second trend due to monodimensional branches for $r > r_C$, where r_C is the radius of the core structure. The second trend can be computed analytically via an integral curve for $N(r > r_C)$ which can be approximated by a power law r^γ ($\gamma = 0.947 \pm 0.002$; see SM Sec. V [44]), as in Ref. [22]. The curve of $N(r)$ is consistent with the real network and confirms scaling laws prediction from Ref. [22].

VII. DISCUSSION

Starting from simple conditions on temporal efficiency on a spatial network substrate, we show that network optimization paired with flows weighting the importance of specific connections in space can reproduce complex networks features from manmade transportation networks. Specifically, we devise a framework for spatial networks where nodes can encode features of urban systems and can ultimately lead to the study of optimal topologies in real scenarios. A key novelty lies in the optimization process happening on a spatial substrate, such that edges' speeds of the resulting optimal network are optimized to improve the efficiency of the shared space by all nodes in the network. We show how distance-based probabilities of moving from one point to another in space force a transition between a treelike and a latticelike topology in the optimal network. Functional dependencies other than exponential decays, such as a power-law decay, may represent future modeling pursuits.

We then investigate the effect of traffic routing during the optimization process following user equilibrium principles, to capture realistic travel behaviors and congestion effects. We introduce this modeling element to analyze how it affects the optimal network structures emerging in simple triangular lattices, providing an analytical derivation of the transition from tree structures to n multiple pathways alternative.

Fixing certain target points in space with a higher attractiveness for flows can reproduce theoretical results such as the Steiner tree solution or leaves venation patterns. We also show that extending these probabilities using urban spatial information and flows with patterns typical of mobility in cities forces the emergence of shared preferential paths that are organized as complex topologies, resulting from flow-weighted optimization of network time efficiency, which ultimately exhibits the characteristics seen in real systems. We recover features such as a bimodality in the speed distribution of the edges of the network, characteristic of multilayer transportation. Or we observe the appearance of a central core with loops coupled

to branches typical of underground systems, as in the case of the London underground system. We find that branches paired to large loops structures appear as optimal structures when the network is optimized for an interplay of traffic flows mixed between small range travels and longer-range ones typical of commuting. Finally, extension of this modeling to other cities represents possible future research. We emphasize that this framework is not primarily intended for a direct urban planning application, but rather represents a network science investigation of optimal transportation networks, encompassing typical urban features. However, this novel framework for the optimization of spatial networks in urban contexts may show further extensions to better accommodate concepts of multilayer network and other aspects in urban planning research. Moreover, it has the potential to be adjusted to provide guidance on the optimal expansion of an existing transit network. It could be extended also to the case of intercities transportation, where specific nodes in the network substrate represent cities. To conclude, in this work the problem is addressed in a theoretical way with the aim of reproducing and understanding some features observed in real spatial networks, but future works can exploit this framework as a basis to understand how to generate optimal transportation networks in an urban planning scenario.

The data used in this work are publicly available from the original references. The code to perform the analysis is available upon request. OpenStreetMap data is available under Open Database License.

ACKNOWLEDGMENTS

M. D. D. acknowledges partial financial support from MUR funding within the FIS (DD n. 1219 31-07-2023) Project no. FIS00000158. B. L. and R. G. acknowledge the support of the PNRR ICSC National Research Centre for High Performance Computing, Big Data and Quantum Computing (CN00000013), under the NRRP MUR program funded by the NextGenerationEU. G. C. acknowledges the support of the European Union's Horizon 2020 research and innovation program under the Marie Sklodowska-Curie Grant Agreement No. 101103026. The authors thank M. Barthelemy for useful discussions.

The authors declare no competing financial interests.

[1] M. Batty, *The size, scale, and shape of cities*, Science **319**, 769 (2008).
[2] M. Barthelemy, *The statistical physics of cities*, Nat. Rev. Phys. **1**, 406 (2019).
[3] L. Bettencourt and G. West, *A unified theory of urban living*, Nature (London) **467**, 912 (2010).
[4] W. Pan, G. Ghoshal, C. Krumme, M. Cebrian, and A. Pentland, *Urban characteristics attributable to density-driven tie formation*, Nat. Commun. **4**, 1961 (2013).
[5] E. Arcaute, E. Hatna, P. Ferguson, H. Youn, A. Johansson, and M. Batty, *Constructing cities, deconstructing scaling laws*, J. R. Soc. Interface **12**, 20140745 (2015).
[6] L. M. A. Bettencourt, *The origins of scaling in cities*, Science **340**, 1438 (2013).
[7] A. Bassolas, H. Barbosa-Filho, B. Dickinson, X. Dotiwalla, P. Eastham, R. Gallotti, G. Ghoshal, B. Gipson, S. A. Hazarie, H. Kautz, O. Kucuktunc, A. Lieber, A. Sadilek, and J. J. Ramasco, *Hierarchical organization of urban mobility and its connection with city livability*, Nat. Commun. **10**, 4817 (2019).
[8] L. M. A. Bettencourt, *Urban growth and the emergent statistics of cities*, Sci. Adv. **6**, eaat8812 (2020).
[9] M. Schläpfer, L. Dong, K. O'Keeffe, P. Santi, M. Szell, H. Salat, S. Anklesaria, M. Vazifeh, C. Ratti, and G. B. West, *The universal visitation law of human mobility*, Nature (London) **593**, 522 (2021).
[10] H. Barbosa, M. Barthelemy, G. Ghoshal, C. R. James, M. Lenormand, T. Louail, R. Menezes, J. J. Ramasco, F. Simini, and M. Tomasini, *Human mobility: Models and applications*, Phys. Rep. **734**, 1 (2018).
[11] L. Alessandretti, L. G. N. Orozco, M. Saberi, M. Szell, and F. Battiston, *Multimodal urban mobility and multilayer transport networks*, Environ. Plan. B **50**, 2038 (2023).
[12] M. Lee, H. Barbosa, H. Youn, P. Holme, and G. Ghoshal, *Morphology of travel routes and the organization of cities*, Nat. Commun. **8**, 2229 (2017).
[13] R. Gallotti, P. Sacco, and M. D. Domenico, *Complex urban systems: Challenges and integrated solutions for the sustainability and resilience of cities*, Complexity **2021**, 1 (2021).
[14] M. Barthélemy, *Spatial networks*, Phys. Rep. **499**, 1 (2011).
[15] R. G. Morris and M. Barthelemy, *Transport on coupled spatial networks*, Phys. Rev. Lett. **109**, 128703 (2012).
[16] M. T. Gastner and M. E. J. Newman, *Optimal design of spatial distribution networks*, Phys. Rev. E **74**, 016117 (2006).
[17] M. Barthélemy and A. Flammini, *Optimal traffic networks*, J. Stat. Mech. 2006, L07002 (2006).
[18] R. Louf, P. Jensen, and M. Barthelemy, *Emergence of hierarchy in cost-driven growth of spatial networks*, Proc. Natl. Acad. Sci. U.S.A. **110**, 8824 (2013).
[19] J. R. Banavar, A. Maritan, and A. Rinaldo, *Size and form in efficient transportation networks*, Nature (London) **399**, 130 (1999).
[20] A. Pei, F. Xiao, S. Yu, and L. Li, *Efficiency in the evolution of metro networks*, Sci. Rep. **12**, 8326 (2022).
[21] R. Gallotti and M. Barthelemy, *The multilayer temporal network of public transport in Great Britain*, Sci. Data **2**, 1 (2015).
[22] C. Roth, S. M. Kang, M. Batty, and M. Barthelemy, *A long-time limit for world subway networks*, J. R. Soc. Interface **9**, 2540 (2012).
[23] A. Tero, S. Takagi, T. Saigusa, K. Ito, D. P. Bebber, M. D. Fricker, K. Yumiki, R. Kobayashi, and T. Nakagaki, *Rules for biologically inspired adaptive network design*, Science **327**, 439 (2010).

[24] R. Louf and M. Barthelemy, *How congestion shapes cities: From mobility patterns to scaling*, Sci. Rep. **4**, 5561 (2014).
[25] E. Taillanter and M. Barthelemy, *Evolution of road infrastructure in large urban areas*, Phys. Rev. E **107**, 034304 (2023).
[26] A. A. Ibrahim, A. Lonardi, and C. D. Bacco, *Optimal transport in multilayer networks for traffic flow optimization*, Algorithms Mol. Biol. **14**, 189 (2021).
[27] M. Dahlmanns, F. Kaiser, and D. Witthaut, *Optimizing the geometry of transportation networks in the presence of congestion*, Phys. Rev. E **108**, 044302 (2023).
[28] X. Zhang, A. Adamatzky, F. T. Chan, Y. Deng, H. Yang, X.-S. Yang, M.-A. I. Tsompanas, G. C. Sirakoulis, and S. Mahadevan, *A biologically inspired network design model*, Sci. Rep. **5**, 1 (2015).
[29] Y. Sheffi, *Urban Transportation Networks*, Vol. 6 (Prentice-Hall, Englewood Cliffs, NJ, 1985).
[30] R. Z. Farahani, E. Miandoabchi, W. Y. Szeto, and H. Rashidi, *A review of urban transportation network design problems*, Eur. J. Oper. Res. **229**, 281 (2013).
[31] S. Patwardhan, M. Barthelemy, S. Erkol, S. Fortunato, and F. Radicchi, *Symmetry breaking in optimal transport networks*, arXiv:2311.05059.
[32] M. J. Nieuwenhuijsen, *Urban and transport planning pathways to carbon neutral, liveable and healthy cities: A review of the current evidence*, Environ. Int. **140**, 105661 (2020).
[33] M. Szell, S. Mimar, T. Perlman, G. Ghoshal, and R. Sinatra, *Growing urban bicycle networks*, Sci. Rep. **12**, 6765 (2022).
[34] V. Morandi, *Bridging the user equilibrium and the system optimum in static traffic assignment: A review*, 4OR, 1 (2023).
[35] Y. Sheffi and W. Powell, *A comparison of stochastic and deterministic traffic assignment over congested networks*, Transp. Res. Part B **15**, 53 (1981).
[36] C. Wei, Y. Asakura, and T. Iryo, *Formulating the within-day dynamic stochastic traffic assignment problem from a Bayesian perspective*, Transp. Res. Part B **59**, 45 (2014).
[37] C. P. Birch, S. P. Oom, and J. A. Beecham, *Rectangular and hexagonal grids used for observation, experiment and simulation in ecology*, Ecol. Model. **206**, 347 (2007).
[38] R. Gallotti, A. Bazzani, S. Rambaldi, and M. Barthelemy, *A stochastic model of randomly accelerated walkers for human mobility*, Nat. Commun. **7**, 12600 (2016).
[39] Y. Ren, M. Ercsey-Ravasz, P. Wang, M. C. González, and Z. Toroczkai, *Predicting commuter flows in spatial networks using a radiation model based on temporal ranges*, Nat. Commun. **5**, 5347 (2014).
[40] A. Wilson, *Some new forms of spatial interaction model: A review*, Transp. Res. **9**, 167 (1975).
[41] M. P. Viana, E. Strano, P. Bordin, and M. Barthelemy, *The simplicity of planar networks*, Sci. Rep. **3**, 3495 (2013).
[42] M. Newman, *Networks* (Oxford University Press, New York, 2010).
[43] T. Kavitha, K. Mehlhorn, D. Michail, and K. E. Paluch, *An algorithm for minimum cycle basis of graphs*, Algorithmica **52**, 333 (2008).
[44] See Supplemental Material at http://link.aps.org/supplemental/10.1103/PhysRevX.14.021050 for additional details regarding the model application on lattices, the GLA network, and the study of congestion dynamics.
[45] E. Katifori, G. J. Szöllősi, and M. O. Magnasco, *Damage and fluctuations induce loops in optimal transport networks*, Phys. Rev. Lett. **104**, 048704 (2010).
[46] F. Simini, M. C. González, A. Maritan, and A.-L. Barabási, *A universal model for mobility and migration patterns*, Nature (London) **484**, 96 (2012).
[47] S. Grauwin, M. Szell, S. Sobolevsky, P. Hövel, F. Simini, M. Vanhoof, Z. Smoreda, A.-L. Barabási, and C. Ratti, *Identifying and modeling the structural discontinuities of human interactions*, Sci. Rep. **7**, 46677 (2017).
[48] O. Cabanas-Tirapu, L. Danús, E. Moro, M. Sales-Pardo, and R. Guimerà, *Human mobility is well described by closed-form gravity-like models learned automatically from data*, arXiv:2312.11281.
[49] D. Piovani, C. Molinero, and A. Wilson, *Urban retail location: Insights from percolation theory and spatial interaction modeling*, PLoS One **12**, e0185787 (2017).
[50] M. Mazzoli, A. Molas, A. Bassolas, M. Lenormand, P. Colet, and J. J. Ramasco, *Field theory for recurrent mobility*, Nat. Commun. **10**, 3895 (2019).
[51] S. E. Dreyfus and R. A. Wagner, *The Steiner problem in graphs*, Networks **1**, 195 (1971).
[52] M. Brazil, R. L. Graham, D. A. Thomas, and M. Zachariasen, *On the history of the Euclidean Steiner tree problem*, Arch. Hist. Exact Sci. **68**, 327 (2013).
[53] C. A. Hidalgo, E. Castañer, and A. Sevtsuk, *The amenity mix of urban neighborhoods*, Habitat Int. **106**, 102205 (2020).
[54] OpenStreetMap contributors, Planet dump retrieved from https://planet.osm.org, https://www.openstreetmap. org.
[55] Uber H3, 2024 Uber Technologies, https://h3geo.org/.